CHIRAL DISORDER AND RANDOM MATRIX THEORY WITH MAGNETISM*

Maciej A. Nowak[a,b,†], Mariusz Sadzikowski[a,‡], Ismail Zahed[c,§]

[a]The Marian Smoluchowski Institute of Physics
Jagiellonian University, Łojasiewicza 11, 30-348 Kraków, Poland
[b]Mark Kac Center for Complex Systems Research
Jagiellonian University, Łojasiewicza 11, 30-348 Kraków, Poland
[c]Department of Physics and Astronomy, Stony Brook University
Stony Brook, New York 11794-3800, USA

We revisit the concept of chiral disorder in QCD in the presence of a QED magnetic field $|eH|$. Weak magnetism corresponds to $|eH| \leq 1/\rho^2$ with $\rho \approx 1/3$ fm the vacuum instanton size, while strong magnetism the reverse. Asymptotics (ultra-strong magnetism) is in the realm of perturbative QCD. We analyze weak magnetism using the concept of the quark return probability in the diffusive regime of chiral disorder. The result is in agreement with expectations from chiral perturbation theory. We analyze strong and ultra-strong magnetism in the ergodic regime using random matrix theory including the effects of finite temperature. The strong magnetism results are in agreement with the currently reported lattice data in the presence of a small shift of the Polyakov line. The ultra-strong magnetism results are consistent with expectations from the perturbative QCD. We suggest a chiral random matrix effective action with matter and magnetism to analyze the QCD phase diagram near the critical points under the influence of magnetism.

1. Introduction

Chiral quarks in the QCD vacuum break spontaneously chiral symmetry. Key contributors to this spontaneous breaking are instanton and anti-instanton fluctuations with left-handed and right-handed zero modes attached to them [1–3] (and references therein). The random nature of the

---

† nowak@th.if.uj.edu.pl

‡ sadzikowski@th.if.uj.edu.pl

§ zahed@tonic.physics.sunysb.edu

instanton and anti-instanton fluctuations causes these zero modes to spread near zero virtuality. This fundamental property of the QCD quark spectrum is captured by the Banks–Casher relation [4]

$$\left\langle \boldsymbol{\Psi}_4^\dagger \boldsymbol{\Psi}_4 \right\rangle \equiv \Sigma_4 = \pi \rho_4(0) \tag{1}$$

that ties the quark condensate to the quark spectral density $\rho_4(\lambda)$ at zero virtuality. Note the positive convention for the chiral condensate. In the QCD vacuum with instanton density $\boldsymbol{n}_4$ and size ρ, the quark condensate is expected to scale as $\Sigma_4 \approx \sqrt{\boldsymbol{n}_4}/\rho$. Using the Gell-Mann–Oakes–Renner relation $m_\pi^2 F_\pi^2 = 2m\Sigma_4$, (1) is just the analogue of the Kubo formula for the DC conductivity in metals

$$\sigma_C = F_\pi^2/\pi = D\rho_4(0) \,. \tag{2}$$

The pion decay constant F_π defines the chiral conductivity, with the chiral diffusion constant $D = F_\pi^2/\Sigma_4$ [3, 5]. Through (1)–(2) chiral quarks trapped in an Euclidean 4-volume $V_4 = L^4$ behave much like electrons in disordered metallic grains with $\lambda_\mathrm{T} = D/L^2$ playing the role of the Thouless energy [5–8]. Quarks with virtualities $\lambda < \lambda_\mathrm{T}$ are in the ergodic regime and are well-described by random matrix theory, while quarks with virtualities $\lambda > \lambda_\mathrm{T}$ are in the diffusive regime which is amenable to chiral perturbation theory. One may also say that in the ergodic regime, the wavelength of the pion is substantially larger than the size of the box, so only the lowest mode (zero mode) is relevant, whereas in the diffusive regime, all pionic modes have to be taken into account, corresponding to chiral perturbation theory regime. In the presence of a fixed external magnetic field H, the chiral disorder is affected. In this paper, we address the details of these changes.

Weak magnetism is mainly affecting the diffusive properties of chiral fermions through a renormalization of the low-energy parameters, e.g. Σ_4, F_π, m_π. Although the chiral expansion in the massless limit relies on $|eH|/(4\pi F_\pi)^2 < 1$ and, therefore, suggests that weak magnetism operates in the realm of $|eH| \le 1\,\mathrm{GeV}^2$, the validity range is substantially smaller. Indeed, since instantons may be at the origin of the spontaneous breaking of chiral symmetry, we expect weak magnetism to break down when the instanton size ρ is resolved. As a result, the range of weak magnetism is $|eH| \le 1/\rho^2 \approx 1/3\,\mathrm{GeV}^2$ and will be referred to as diffusive.

Strong magnetism corresponds to $|eH| > 1/\rho^2 \approx 1/3\,\mathrm{GeV}^2$ with a magnetic field starting to dwarf the chromomagnetic field carried by the instanton. This range will be referred to as ergodic. As a result, light and chiral quarks in the QCD vacuum switch from locking their spin to the instanton color to lining their spin with the external magnetic field. They

form Landau orbits which are gapped by $|eH|$ near zero virtuality. The exception is the lowest Landau level (or LLL for short), where the magnetic contribution cancels the zero point motion. As a result, the LLL with its huge degeneracy piles up at zero virtuality becoming a potential contributor to the spontaneous breaking of chiral symmetry. The LLL is inherently 2-dimensional. This phenomenon of dimensional reduction from 4 to 2 in Euclidean space with accumulation near zero virtuality of the LLL favors the spontaneous breaking of chiral symmetry through any residual interaction. This phenomenon is known as magnetic catalysis [9] (and references therein). For instance, residual longitudinal interactions in the LLL through the instantons will cause the spontaneous breaking of chiral symmetry

$$\Sigma_4 = |eH|\Sigma_2 \approx |eH|\sqrt{n_4}\rho \tag{3}$$

with typically $\boldsymbol{n_4} \approx 1/\text{fm}^4$ the vacuum instanton density.

Ultra-strong magnetism is solely characterized by Landau levels with huge degeneracy and small sizes. As a result, many Landau orbits can fit in a single instanton making the concept of instanton zero modes not particularly useful. In many ways, this picture resembles that of the initial color glass condensate with many wee partons saturating the transverse size of a colliding nucleus [10] (and references therein). Perturbation theory becomes the rule and will cause the LLL to spread near zero virtuality. The spontaneous breaking of chiral symmetry through perturbative gluons follows with

$$\Sigma_4 = |eH|\Sigma_2 \approx |eH|^{3/2} \tag{4}$$

as expected from dimensional arguments. We expect this scaling to take place for $|eH| \geq 10/\rho^2 \approx 3\,\text{GeV}^2$ or when about 10 Landau orbits can fit within the instanton transverse size dwarfing thereby the zero modes. Both strong and ultra-strong regimes belong to the realm of random matrix theory, albeit they are described by different random matrix models. In Section 2, we discuss weak magnetism in the diffusive regime of 4-dimensional chiral quarks trapped in V_4 using the concept of the quark return probability. The result is in line with the one from chiral perturbation theory. In Sections 3 and 4, we discuss ultra-strong and strong magnetism in the ergodic regime where the instanton size is resolved through the use of random matrix theory. The results are in line with the expectations of dimensional reduction from the LLL. In Section 5, we compare our results to current lattice simulations [11, 12]. In particular, we show that a small shift in the trivial Polyakov holonomy is magnified by the chiral transition and may account for the anti-catalysis observed on the lattice as recently suggested in [13]. In Section 6, we show how random matrix models for QCD with magnetism

can be constructed to shed light on the comparison with widely used constituent quark models of the NJL type, and help analyze a number of issues in the QCD phase diagram with magnetism. Our conclusions and prospects are in Section 7.

2. Diffusive regime with weak magnetism

The dynamics of QCD light quarks in a 4-dimensional Euclidean box is chiral and diffusive in the long wavelength limit. The diffusive nature is best captured by the quark return probability [5]

$$P(0,\tau) = \left\langle \left| u^+(\tau)u(0) + d^+(\tau)d(0) \right|^2 \right\rangle \tag{5}$$

for 2 light flavors. In the absence of magnetism, the vacuum is isospin symmetric and (5) is dominated by the triplet of pions in an Euclidean box

$$P(0,\tau) = 2\left(P_0(0,\tau) + P_\pm(0,\tau) \right) \tag{6}$$

with

$$P_{0,\pm}(0,\tau) \approx \sum_Q e^{-DQ^2|\tau|} \tag{7}$$

for a triplet of massless pions. The sum is over the isotriplet of charged pions or diffuson modes with momenta $Q_\mu = n_\mu 2\pi/L$ in a periodic $V_4 = L^4$ Euclidean box. The quark return probability (5) in the chiral limit obeys a sum rule

$$\Sigma_4 = -\lim_{m\to 0} \lim_{V_4\to\infty} \frac{1}{V_4} \int\limits_0^\infty P(0,\tau)\,\mathrm{d}\tau\,. \tag{8}$$

In the presence of magnetism, the vacuum is no longer isospin symmetric. As a result, the free chargeless pion π^0 remains gapless, while the free charged pions $\pi^\pm$ are gapped in Landau levels (LL). For a constant magnetic field with $A^1 = -Hx_2$, the LL are

$$\lambda_\pm^2 = |eH|(2n+1) + p_3^2 + p_4^2 + m_\pm^2 \tag{9}$$

with degeneracy $\phi = eHL^2/2\pi$. The change in the quark return probability follows from the change in the diffuson propagator for the charged pion modes

$$P_\pm(H,\tau) = \sum_{n,m,k} \frac{eHL^2}{2\pi} e^{-D\tau\left[(n+1/2)2eH + (m^2+k^2)(2\pi/L)^2 + m_\pm^2\right]}\,. \tag{10}$$

The change in the quark return probability is the change in the charged diffuson modes and is captured by the difference

$$I = \int_0^\infty [P_\pm(H,\tau) - P_\pm(0,\tau)]\,d\tau\,. \tag{11}$$

In the chiral limit, replacing the sums over free momenta by integrals and summing explicitly over the Landau levels of the charged pions (*i.e.* the diffusons), we obtain

$$I = \frac{eHV}{16\pi^2 D} \int_0^\infty \left(\frac{1}{z\sinh z} - \frac{1}{z^2}\right) dz = -\frac{eHV}{16\pi^2 D}\ln 2\,. \tag{12}$$

Using the value of the diffusion constant, we arrive at

$$\Sigma_4(H) = \Sigma_4(0)\left(1 + \frac{eH\ln 2}{16\pi^2 F_\pi^2}\right) \tag{13}$$

which is the result of chiral perturbation theory in leading order [14]. As expected, the diffusive regime is the regime of chiral perturbation theory albeit in a finite Euclidean box [15]. Chiral perturbation theory in a finite box was formulated systematically in [16].

3. Ergodic regime with ultra-strong magnetism

For strong magnetism, the chiral disorder in 4 dimensions with an iso-triplet of pions transmute to a chiral disorder in quasi-2 dimensions with a chargeless pion, as the charged diffusons become gapped. The transmutation takes place when the magnetic field resolves the instanton size or $|eH| > 1/\rho^2 \approx 1/3\,\text{GeV}^2$. In this regime, magnetism dwarfs the instanton chromo-magnetism with Landau levels becoming the lore. The LLL dominates the infrared physics near zero virtuality triggering the catalysis of chiral symmetry breaking by magnetism.

Indeed, for strong magnetism, the free quark spectrum in 4 dimensions is given by Landau levels

$$\lambda_{n,s}^\pm(\omega, k_z) = \pm\sqrt{\omega^2 + k_z^2 + |eH|(2n+1-s) + m^2} \tag{14}$$

with current quark masses. For simplicity, we will consider $N_F = 1$ with charge e unless specified otherwise. Each (ω, k_z) branch is

$$\phi = |eH|L_x L_y/2\pi \equiv |H|L_x L_y/(hc/e) \tag{15}$$

degenerate. (15) measures the magnetic flux in units of the quantum flux hc/e and is integer valued on a 4-dimensional lattice with periodic (toroidal) boundary conditions. The lowest Landau branches $n = 0$, $s = 1$

$$\lambda_{0,1}^{\pm}(\omega, k_z) = \pm\sqrt{\omega^2 + k_z^2 + m^2} \qquad (16)$$

are paired by chirality and dominate in the infrared limit. They are 2ϕ degenerate. The higher Landau levels are gapped at zero virtuality. We note that at finite temperature, the ω-spectrum in (16) is dominated by the lowest Matsubara mode $\omega \to \omega_0 = \pi T$ [17]. This approximation will be used to probe critical points in phase diagrams with magnetism.

While the color interactions are involved within and between Landau levels, a model-independent understanding can be achieved through the Banks–Casher formula used earlier. In the presence of strong magnetism, the localization of the quark spectrum in the transverse hyperplane to the magnetic field suggests

$$\left\langle \Psi_4^{\dagger}\Psi_4 \right\rangle = \pi\rho_4(0) = \frac{\pi}{V_4}\frac{2\phi}{\Delta\lambda} = \frac{|eH|}{\beta L_z\Delta\lambda}\,, \qquad (17)$$

where $\Delta\lambda$ is the typical level spacing near zero virtuality. In a spontaneously broken QCD vacuum with no magnetism, $\Delta\lambda \approx 1/V_4$. The last relation in (17) reflects on the dimensional reduction of the quark spectral function near zero virtuality from 4 to 2 dimensions

$$\rho_4(0) = |eH|\rho_2(0) \qquad (18)$$

and, therefore, the condensate relation

$$\left\langle \Psi_4^{\dagger}\Psi_4 \right\rangle = |eH| \left\langle \Psi_2^{\dagger}\Psi_2 \right\rangle \,. \qquad (19)$$

In the infrared regime, this suggests the field redefinition

$$\Psi_4(x_0, x, y, z)) \to \sqrt{|eH|}\,\Psi_2(x_0, z) \qquad (20)$$

with the pertinent canonical dimensions made explicit.

The breaking of chiral symmetry in terms of $\boldsymbol{\Psi}_2$ is quasi-2-dimensional. It does not upset the Mermin–Wagner theorem. Indeed, the random gluonic interactions that cause the spontaneous breaking of chiral symmetry and, therefore, the redistribution of the 2-dimensional quark spectrum near zero virtuality are still blind to magnetism and fully 4-dimensional.

In quasi-2 dimensions, the free quark fields Ψ_2 are dominated by the branches (16) and any residual gluonic interaction will cause them to redistribute. For ultra-strong magnetism with

$$|eH| \geq 10/\rho^2 \approx 3\,\text{GeV}^2\,,$$

the interactions among the quarks in the LLL are mainly perturbative as the instanton quasi-zero modes become obsolete. Assuming the residual interactions in the infrared for the lowest Landau level (LLL) and lowest Matsubara frequency to be totally random but chiral, the partition function for these modes is best captured by a new chiral RMM

$$\boldsymbol{Z}_{\text{LLL}}(m, T, \phi) = \int \mathrm{d}\boldsymbol{A} \, e^{-(\phi/|eH|)\text{Tr}(\boldsymbol{A}^\dagger \boldsymbol{A})} \, \det \begin{vmatrix} m & i\omega_0 + i\boldsymbol{A} \\ i\omega_0 + i\boldsymbol{A}^\dagger & m \end{vmatrix},$$
(21)

where $\boldsymbol{A}$ is a $\phi \times \phi$ complex matrix with a Gaussian distribution. Recall that we have set $N_F = 1$. The novelty of (21) is in the scaling of the Gaussian distribution of the matrix elements with magnetism. It captures the random interactions induced by plain perturbative gluons between the ϕ degenerate quarks $\boldsymbol{\Psi}_2$ in the LLL and amounts to the 4-Fermi interaction

$$|eH| \left(\boldsymbol{\Psi}_2^\dagger \boldsymbol{\Psi}_2 \right)^2$$

as expected from dimensional reduction. The Gaussian weight enforces a level spacing between the eigenvalues of the chiral matrix to be of the order of

$$\Delta\lambda \sim \frac{\sqrt{|eH|}}{\phi} \,.$$
(22)

By the Banks–Casher formula, we expect the chiral condensate in a symmetric box $V_4 = L^4$

$$\left\langle \Psi_4^\dagger \Psi_4 \right\rangle = \pi\rho_4(0) = \frac{\pi}{V_4} \frac{2\phi}{\Delta\lambda} \sim \frac{1}{2\pi} |eH|^{3/2}$$
(23)

which is in agreement with the dimensional arguments presented in (4). This result is born out by explicit calculations as we now show.

The quark condensate follows through (19) as

$$\left\langle \Psi_4^\dagger \Psi_4 \right\rangle = \lim_{m \to 0} \frac{|eH|}{\beta L_z} \frac{\partial \ln \boldsymbol{Z}_{\text{LLL}}}{\partial m} \,.$$
(24)

In the large ϕ limit, the partition function in (24) is analyzed through standard arguments by fermionizing the determinant in (21), performing the Gaussian integral and then bosonizing the resulting 4-Fermi interaction using the Hubbard–Stratonovitch transform

$$Z_{\text{LLL}}(m, T, \phi) = \int \mathrm{d}\boldsymbol{b} \, e^{-\frac{\phi}{|eH|}\boldsymbol{b}^\dagger \boldsymbol{b}} \, \det^\phi \begin{vmatrix} \boldsymbol{b} + m & i\omega_0 \\ i\omega_0 & \boldsymbol{b}^\dagger + m \end{vmatrix} \,.$$
(25)

Inserting (25) into (24) yields

$$\left\langle \boldsymbol{\Psi}_4^\dagger \boldsymbol{\Psi}_4 \right\rangle = \lim_{m \to 0} \lim_{L_z \to \infty} \frac{|eH|}{\beta L_z} \left\langle \mathrm{Tr} \begin{vmatrix} \boldsymbol{b} + m & i\omega_0 \\ i\omega_0 & \boldsymbol{b}^\dagger + m \end{vmatrix}^{-1} \right\rangle . \tag{26}$$

The averaging is carried using the measure in (25). In the saddle point approximation, the result is

$$\left\langle \Psi_4^\dagger \Psi_4 \right\rangle = \frac{|eH|}{\beta L_z} \frac{2\phi}{\sqrt{|eH|}} \sqrt{1 - \omega_0^2/|eH|} \tag{27}$$

which can be re-written as

$$\left\langle \Psi_4^\dagger \Psi_4 \right\rangle = \frac{L_x L_y}{\beta L_z} \frac{1}{\pi} |eH|^{3/2} \sqrt{1 - \omega_0^2/|eH|} \tag{28}$$

which is (23) for a symmetric box. The critical temperature is field-dependent

$$T_{\mathrm{c}} = \frac{\sqrt{|eH|}}{\pi} . \tag{29}$$

Ultra-strong magnetism implies tightly paired chiral quarks in the vacuum. The RMM results (23) and (29) are consistent with dimensional arguments for asymptotically strong magnetism, and the perturbative QCD arguments presented in [14]. This analysis ignores the back-reaction of the quarks on the gauge configurations in the saddle point approximation. The back-reaction maybe important as we detail below.

Finally, we note that a more general RMM for all Landau levels can be written similarly by insisting on the free Landau level spectrum for $\boldsymbol{A} = 0$. Specifically,

$$\boldsymbol{Z}_{\mathrm{LL}}(m, T, \phi) = \int \mathrm{d}\boldsymbol{A}\, e^{-(\phi/|eH|)\mathrm{Tr}(\boldsymbol{A}^\dagger \boldsymbol{A})} \prod_{n=0}^{\infty} \prod_{s=\pm 1}$$
$$\times \det \begin{vmatrix} m & i\omega_0 + \epsilon(n, s) + i\boldsymbol{A} \\ i\omega_0 - \epsilon(n, s) + i\boldsymbol{A}^\dagger & m \end{vmatrix} \tag{30}$$

with the free Landau level eigenvalue-spectrum

$$\omega_0^2 + \epsilon^2(n, s) + m^2 = \omega_0^2 + |eH|(2n + 1 - s) + m^2 . \tag{31}$$

(21) is (30) restricted to the LLL with $n = 0$, $s = 1$. Other matrix models with cross LL interactions are also possible, although suppressed by the large $|eH|$ gap between LL.

4. Ergodic regime with strong magnetism

For strong QED magnetic fields with a running coupling $g(eH)$ that is not so small, the semi-classical configurations such as instantons (vacuum) or calorons (thermal) are not suppressed. Although 4-dimensional, these configurations may considerably interact with the dimensionally reduced quark fields $\boldsymbol{\Psi}_2$ and localize them in near-zero modes. A recent discussion of these near-zero modes for a single instanton configuration can be found in [18]. Let N be the number of these near-zero modes in the transverse hyperplane to the magnetic field. Since the chiralities in 4 dimensions are commensurate with the chiralities in 2 dimensions, the pertinent chiral RMM for these near-zero modes is then standard

$$\boldsymbol{Z}_{\mathrm{LLL}}(m, T, \Lambda) = \int \mathrm{d}\boldsymbol{A}\, e^{-(N/\Lambda^2)\mathrm{Tr}(\boldsymbol{A}^\dagger \boldsymbol{A})}\, \det \begin{vmatrix} m & i\omega_0 + i\boldsymbol{A} \\ i\omega_0 + i\boldsymbol{A}^\dagger & m \end{vmatrix} \quad (32)$$

with $\boldsymbol{A}$ an $N \times N$ matrix and $\Lambda \approx 1/\rho$ a typical QCD scale set by the instanton size ρ for instance. The Gaussian weighting in (32) induces a 4-Fermi interaction

$$\Lambda^2 \left(\boldsymbol{\Psi}_2^\dagger \boldsymbol{\Psi}_2 \right)^2$$

for the dimensionally reduced quarks. Note that the level spacing of the $\boldsymbol{\Psi}_2$ is

$$\Delta\lambda \sim \frac{\Lambda}{N} \quad (33)$$

instead of (22). Again, by the Banks–Casher formula, we expect the chiral condensate in a symmetric box to scale as

$$\left\langle \Psi_4^\dagger \Psi_4 \right\rangle = \pi\rho(0) = \frac{\pi}{V_4}\frac{2\phi}{\Delta\lambda} \sim \frac{|eH|}{\Lambda}\frac{N}{\sqrt{V_4}} \quad (34)$$

with $\boldsymbol{n}_4 = N^2/V_4 \approx 1/\mathrm{fm}^4$ as typically the instanton–anti-instanton density in the QCD vacuum.

The chiral condensate follows through similar reasoning at the saddle point for large N and at finite temperature

$$\left\langle \Psi_4^\dagger \Psi_4 \right\rangle = \frac{2N}{\beta L_z}\frac{|eH|}{\Lambda}\sqrt{1 - \omega_0^2/\Lambda^2}\,. \quad (35)$$

$N/\beta L_z$ is about the number of instantons and anti-instantons in βL_z regarded as a slice of $V_4 = \beta L_x L_y L_z$. This is roughly $\sqrt{\boldsymbol{n}_4}$ since the instanton density $\boldsymbol{n}_4$ varies slowly with temperature except for $T \approx T_{\mathrm{c}}$, where a

re-arrangement into pairs is expected. Thus, the spacing (33) between the eigenvalues is about $\Delta\lambda \approx 1/\sqrt{V_4}$ in the presence of a strong magnetic field instead of $\Delta\lambda \approx 1/V_4$ in the vacuum.

The chiral condensate is seen to grow linearly with the magnetic field. Unlike the precedent matrix model, the transition temperature is independent of the magnetic field

$$T_c = \Lambda/\pi \,. \tag{36}$$

Therefore, the slope of the chiral condensate for strong magnetism is

$$\left\langle \Psi_4^\dagger \Psi_4 \right\rangle \approx \frac{2\sqrt{\boldsymbol{n}_4}}{\pi T_c} \, |eH| \, \sqrt{1 - (T/T_c)^2} \,. \tag{37}$$

In the RMM, the chiral condensate at zero temperature is fixed by similar arguments. As a result, the relative change of the chiral condensate with magnetism is

$$\Delta\Sigma = \frac{\left\langle \Psi_4^\dagger \Psi_4 \right\rangle}{\left\langle \Psi_4^\dagger \Psi_4 \right\rangle_0} \approx \frac{|eH|}{\sqrt{\boldsymbol{n}_4}} \, \sqrt{1 - (T/T_c)^2} \tag{38}$$

with $\boldsymbol{n}_4 \approx 1/\,\mathrm{fm}^4$ and T_c about the critical temperature for chiral symmetry restoration without magnetism.

We note that the effects of the higher LL on the quark condensate can be readily assessed in the generalized random matrix model (30) in the large ϕ (ultra-strong magnetism) and large N (strong magnetism) limit using the saddle point approximation. Indeed, in the latter limit and retaining the LLL, $n = 0$, $s = 1$ along with the next to lowest LLL $n = 0$, $s = -1$ and $n = 1$, $s = 1$ yield

$$\left\langle \Psi_4^\dagger \Psi_4 \right\rangle = \frac{N}{\beta L_z} \frac{2|eH|}{\Lambda} \left(\sqrt{1 - \omega_0^2/\Lambda^2} + 2\sqrt{1 - 2|eH|/\Lambda^2 - \omega_0^2/\Lambda^2} \right) \,. \tag{39}$$

The next to LLL contribution drops for strong fields or $|eH| > \Lambda^2/2$ as its corresponding saddle point moves off the real axis. Typically, $\Lambda \approx 0.5\,\mathrm{GeV}$ (see below) so that the decoupling takes place for $|eH| \geq 1/3\,\mathrm{GeV}^2$ which is the onset of the ergodic regime. Thus our reduction to the LLL.

5. Comparison with lattice simulations

For intermediate values of $|eH| \leq 1\,\mathrm{GeV}^2$, our results for strong magnetism using random matrix theory and zero temperature are overall consistent with those reported by the recent lattice simulations in [11] and in [19]. The deviations at low values of $|eH| < 1/3\,\mathrm{GeV}^2$ occur in the diffusive

regime and are determined by the pion modes as we detailed earlier through the quark return probability. At finite temperature, our results for strong magnetism using random matrix theory show a field-independent critical temperature (36). The lattice results reported in [11] show a critical temperature weakly dependent on the magnetic field. The critical temperature appears to decrease by about 10% across the critical temperature. An anti-catalysis with a substantial decrease of the chiral condensate was reported to take place close to the critical temperature.

In a recent investigation [13], the breaking of Z_{N_C} symmetry at high temperature with the appearance of a finite Polyakov holonomy was suggested as the mechanism for the appearance of the anti-catalysis phenomenon in the lattice data. The argument is that the finite temporal holonomy $A_4 = \pi \varphi_4 T$ with $\varphi_4 = (0, \pm 2/3) \pmod 2$ for $N_C = 3$ or $\varphi_4 = 0, 1 \pmod 2$ for $N_C = 2$ gets shifted by the magnetic field through sea effects. The result is a decrease of the chiral condensate around the critical temperature. In other words, while the valence contribution is diamagnetic, the sea contribution through the Polyakov holonomy appears to be paramagnetic.

Indeed, a small shift in the trivial Polyakov holonomy by the applied magnetic field can cause the chiral condensate to decrease substantially near the critical temperature. The effect of the Polyakov holonomy is to alter the twisting of the temporal fermionic boundary condition and, therefore, an up or down shift in the Matsubara frequencies. In the LLL, the Polyakov holonomy is readily inserted through

$$
\begin{aligned}
\boldsymbol{Z}_{\mathrm{LLL}}(m, T, A_4) \;=\; & \int \mathrm{d}\boldsymbol{A}\, e^{-(N/\Lambda^2)\mathrm{Tr}(\boldsymbol{A}^\dagger \boldsymbol{A})} \\
& \times \det \begin{vmatrix} m & i(\omega_0 + A_4) + i\boldsymbol{A} \\ i(\omega_0 + A_4) + i\boldsymbol{A}^\dagger & m \end{vmatrix}
\end{aligned}
\tag{40}
$$

instead of (32). The immediate effect of the Polyakov holonomy is to change the onset of the critical temperature to $T_{\mathrm{c}} = (\Lambda/\pi)/|1 + \varphi_4| \pmod 2$ in agreement with the result in [25].

The magnetic shift of the effective potential for the trivial Polyakov holonomy maybe estimated. At high temperature and for massless quarks, the shift in the pressure due to magnetism is [23, 24] (see also Section 6)

$$
\Delta \Omega_H \approx \frac{\chi}{2} |eH|^2 \ln\left(\frac{\omega_0^2}{|eH|}\right)
\tag{41}
$$

with $\chi = N_C/12\pi^2$. In the presence of a finite holonomy, the shift is more subtle to analyze in general. However, for the arguments to follow, it suffices

to assume that generically the holonomy $\varphi \equiv A_4/\omega_0$ shifts away from zero in the presence of magnetism with $\varphi_4(H) \approx \mathcal{O}(e^2)$ as also suggested by current lattice data [13]. Typically,

$$\varphi_4(H) \approx 0 - C\frac{|eH|^2}{\omega_0^4} \qquad (42)$$

with C a parameter to be fixed below. While such a shift is small, it can dramatically affect the chiral condensate near the critical temperature. Indeed, inserting (42) into the random matrix model yields a chiral condensate

$$\left\langle \Psi_4^\dagger \Psi_4 \right\rangle \to \frac{N}{\beta L_z} \frac{2|eH|}{\Lambda} \frac{1}{2} \sum_{s=\pm 1} \sqrt{1 - (T/T_c)^2(s + \varphi_4(H))^2}\,. \qquad (43)$$

The sum over $s = \pm$ signs in (43) is important to understand in our simplified random matrix theory. The chiral condensate in the saddle point approximation receives contribution from **all** Matsubara frequencies $\omega_n = (2n+1)\pi T$ requiring, in principle, a matrix model with all frequencies [3, 25]. Such a matrix model can be written and is explicitly periodic in φ_4 of period 2. However, near the critical points, only the 2 lowest Matubara frequencies are dominant, *i.e.* $\omega_0 = -\omega_{-1}$ (high temperature reduction). In the absence of holonomies, the random matrix model does not distinguish between these 2 frequencies near the critical points, thus the simplification to ω_0. For a finite Polyakov holonomy, the 2 Matsubara frequencies are distinguishable, thus the sum over the signs.

In the random matrix model, the reduction of the chiral condensate takes place when

$$\frac{T_c(H)}{T_c(0)} = \frac{1}{|s + \varphi_4(H)|} \approx 1 - s\varphi_4(H)\,, \qquad (44)$$

where the subscript refers to the critical point. The ω_{-1} contribution in (43) drops first for a critical temperature $T_c(H)/T_c(0) \approx 1 - |\varphi_4(H)|$. Lattice results suggest that the change in the critical temperature $T_c(H)$ with the magnetic field present is about 10% lower than without [11, 12]. Comparison with the lattice data from [12] fixes $C \approx 0.017$ in (42) (see Fig. 1). As a result, (43) reduces at the critical point to

$$\left\langle \Psi_4^\dagger \Psi_4 \right\rangle \to \frac{N}{\beta L_z} \frac{|eH|}{\Lambda} \sqrt{|\varphi_4(H)|}\,(1 - |\varphi_4(H)|) \qquad (45)$$

which is small and vanishes continuously with the increase of magnetism.

We note that (44) implies a critical $H_c(T)$

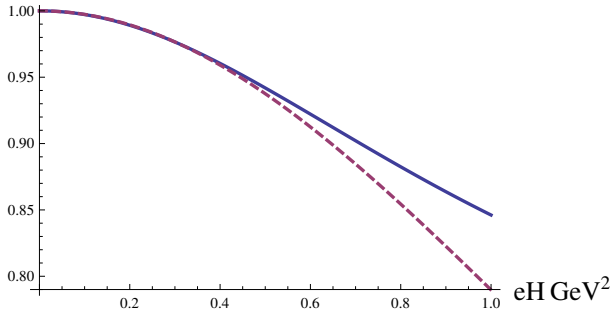$$eH_c(T) \approx \frac{\omega_0^2}{\sqrt{C}} \left(1 - \frac{T}{T_c}\right)^{1/2} \qquad (46)$$

Fig. 1. $T_c(H)/T_c(0)$ as a function of eH. The solid curve describes the fit to the lattice data [12, Eq. (3.1)]. The dashed curve is given by formula (44) with the parameter $C = 0.017$ at $T = T_c(0) = 0.16$ GeV [12].

for the restoration of chiral symmetry at fixed magnetism and finite temperature for $N_c = 3$. This is in qualitative agreement with the reported lattice data. The case of $N_c = 2$ will be adressed in a sequel.

As a final note, we would like to indicate that there is yet another way to test the nature of magnetism on the lattice and that is by twisting the fermionic boundary condition along L_z with a Bohm–Aharonov flux A_z. Specifically,

$$\Psi_2(x_0, z + L_z) = -e^{i2\pi\varphi_z}\Psi_2(x_0, z).\tag{47}$$

This amounts to a bulk Abelian potential [21, 22, 25]

$$(i\gamma \cdot \nabla_E + A_z\gamma_z)\Psi_4 = \lambda[A_z]\Psi_4\tag{48}$$

with a constant $A_z = 2\pi\varphi_z/L_z$. Recall that a constant A_z is physical on a torus. Note that for (48), the quark virtualities $\lambda[A_z]$ are periodic in φ_z of period 1. The twisted boundary condition (47) on the LLL in the random matrix model is achieved by using

$$\det\begin{vmatrix} m & i(\omega_0 + A_4) + A_z + i\boldsymbol{A} \\ i\boldsymbol{A}^\dagger + i(\omega_0 + A_4) - A_z & m \end{vmatrix}\tag{49}$$

in (40). The chiral condensate follows through similar reasoning at the saddle point for large N with

$$\left\langle \Psi_4^\dagger \Psi_4 \right\rangle = \frac{N}{\beta L_z}\frac{2|eH|}{\Lambda}\sqrt{1 - A_z^2/\Lambda^2 - (\omega_0 + A_4)^2/\Lambda^2}\tag{50}$$

instead of (35). At zero temperature, the change in the chiral condensate is

$$\Delta\Sigma = \frac{\left\langle \Psi_4^\dagger \Psi_4 \right\rangle}{\left\langle \Psi_4^\dagger \Psi_4 \right\rangle_0} = \frac{|eH|}{\sqrt{\boldsymbol{n}_4}}\sqrt{1 - A_z^2/\Lambda^2}\,.\tag{51}$$

It would be interesting to carry numerical simulations of spectra and derive the chiral condensate from the pertinent spectral fluctuations using directly the finite size random matrix construction with magnetism. Sea effects can also be analyzed in this way through relevant rescaling limits [20], although the random matrix model is totally dominated by the LLL with or without the Polyakov holonomy in the ergodic regime, as we have discussed. The effects of light quark masses and $N_F > 1$ will be addressed elsewhere.

6. RMM effective action with magnetism

The random matrix effective action with magnetism follows from (30) through standard fermionization of the determinant and then bosonization by the use of the Hubbard–Stratonovitch transformation. The result for the partition function (30) is

$$Z_{\mathrm{LL}}(m, T, \phi) = \int \mathrm{d}\boldsymbol{B}\, e^{-\frac{N}{\Lambda^2}\mathrm{Tr}\,\boldsymbol{B}^\dagger \boldsymbol{B}}\, \det{}^N \begin{vmatrix} \boldsymbol{B} + m & i\boldsymbol{L} \\ i\boldsymbol{L}^\dagger & \boldsymbol{B}^\dagger + m \end{vmatrix} \qquad (52)$$

with

$$\boldsymbol{L} \equiv \left((\omega_0 + A_4) - i\epsilon(n, s)\right)\mathbf{1}_{ns}$$

a diagonal matrix labeling the Landau levels shifted by the lowest Matsubara. The dominant contribution stems from the restriction to the LLL with $\mathbf{1}_{01}$ and corresponds to the reduction $\boldsymbol{\Psi}_4$ to $\boldsymbol{\Psi}_2$. The addition of the spatial twist is straightforward. The corresponding effective action for the LLL in 2 dimensions is

$$\Omega_{\mathrm{LL}} = \frac{N}{\Lambda^2}\,\mathrm{Tr}\,\boldsymbol{B}^\dagger \boldsymbol{B} - N \ln\det \begin{vmatrix} \boldsymbol{B} + m & i\boldsymbol{L} \\ i\boldsymbol{L}^\dagger & \boldsymbol{B}^\dagger + m \end{vmatrix}. \qquad (53)$$

(53) restricted to the LLL describes the dimensionally reduced effective action that describes the quark spectrum near zero virtuality for strong fields in the ergodic regime. For instance,

$$\left\langle \boldsymbol{\Psi}_2^\dagger \boldsymbol{\Psi}_2 \right\rangle = \lim_{m \to 0} \lim_{L_z \to \infty} \frac{N}{\beta L_z} \left\langle \mathrm{Tr} \begin{vmatrix} \boldsymbol{B} + m & i\boldsymbol{L} \\ i\boldsymbol{L}^\dagger & \boldsymbol{B}^\dagger + m \end{vmatrix}^{-1} \right\rangle. \qquad (54)$$

The averaging is carried using the measure in (52). The content of this dimensionally reduced effective action along with the role of a spatial twist and a real quark chemical potential will be discussed elsewhere.

In what follows, we will develop a more phenomenologically inspired random matrix effective action that interpolates between the diffusive and ergodic regime through a reduction of the NJL model to constant modes [3]

(and references therein). The results are inspired chiral RMM effective actions with magnetism. The purpose of this construction is to show the potential relationship between the random matrix theory discussed above as suggested by the mesoscopic analysis and the body of work on magnetism using NJL inspired models.

To analyze the chiral Euclidean effective action or pressure, we recall that the Gibbs energy for finite T and μ of chiral RMM is that of a two-level system for a particle and anti-particle for a single Matsubara frequency and $N_F = 1$ [3, 17]

$$\Omega_M(T,\mu) = \frac{1}{2}\Sigma^2\sigma^2 - \frac{\boldsymbol{n_4}}{2}\ln\left(\left((\sigma-\mu)^2 + (\pi T)^2\right)\left((\sigma+\mu)^2 + (\pi T)^2\right)\right) \quad (55)$$

with σ playing the role of the constituent quark mass and Σ^2 the strength of the chiral Gaussian noise. It ties to the chiral condensate in the vacuum through

$$\left\langle \Psi_4^+\Psi_4 \right\rangle = \Sigma^2\sigma_* \quad (56)$$

at the extremum. Again, the density $\boldsymbol{n_4} = \boldsymbol{N}/V_4$ refers, in general, to the number $\boldsymbol{N}$ of zero modes in the 4-volume which is commensurate with the density of instantons plus anti-instantons in the vacuum.

AB fluxes act as Abelian U(1) vector potentials and are readily implemented in (55) through the substitution

$$(i\mu)^2 \to (i\mu + A_4)^2 + A_z^2. \quad (57)$$

We recall that on a torus, constant gauge fields are gauge invariant. For $\mu = A_4 = T = 0$, (55) simplifies to

$$\Omega_M(A_z) = \frac{1}{2}\Sigma^2\sigma^2 - \frac{\boldsymbol{n_4}}{2}\ln\left(\sigma^2 + A_z^2\right)^2 \quad (58)$$

with a chiral condensate at the minimum

$$\left\langle \boldsymbol{\Psi}_4^\dagger\boldsymbol{\Psi}_4 \right\rangle \equiv \Sigma^2\sigma_* = \Sigma\sqrt{2\boldsymbol{n_4} - (A_z\Sigma)^2} \quad (59)$$

that decreases with the twisting of the boundary condition as we noted earlier.

The virtuality levels of constituent quarks in a fixed external magnetic field along the z-direction are fixed by (14). The vacuum energy follows by summing over the negative energy states through standard procedure. Specifically, the negative of the energy per unit V_4 or pressure reads

$$\Omega_H(0,0) = \frac{H^2}{2} + \frac{|eH|}{(2\pi)^2}\sum_{n=0}^{\infty}\int \mathrm{d}k_z(2 - \delta_{n0})\lambda_{n,1}^-(0,k_z), \quad (60)$$

where we have added the external magnetic field energy density contribution. The sum is UV divergent and requires renormalization. Most importantly, we note that in the vacuum state, all the states are paired in spin with the exception of the state $n = 0$ and $s = 1$. The disordered smearing of this near-threshold state is responsible for the spontaneous breaking of chiral symmetry by strong magnetism as we showed above.

The leading order in $1/N_c$ effects to the free constituent quark loop is the dominant contribution whereby the constituent quark mass is generated through weaker residual and attractive interactions say of the instanton type. For a fixed external magnetic field, the constituent quark loop contributes to the magnetic permittivity $\mu(H)$. For a fixed cut-off Λ_{UV} and a strong magnetic field or $\Lambda_{UV} > \sqrt{|eH|} > (\sigma + m)$ [23]

$$\Omega_H(0,0) \equiv \frac{H^2}{2\mu(H)} \approx \frac{H^2}{2}\left(1 + \chi e^2 \ln\left(\frac{\Lambda_{UV}^2}{eH}\right)\right) \tag{61}$$

for $N_F = 1$. For several quark flavors, $e^2 \to \sum_q^{N_F} e_q^2$ with $N_F = 3$, $e_u = 2e/3, e_d = -e/3, e_s = e/3$. Since the loop contribution stems from the UV sector, the constituent quarks are for all purpose massless, making the logarithmic contribution unique. The plus sign of the vacuum contribution reflects on the diamagnetism and hence the stability of the vacuum state under the switching of a constant H. All the remaining contributions from the loop are analytic in $\mathcal{O}((eH)^2)$ and go into the charge and H renormalization. The combination eH is renormalization group invariant. We set the renormalization so that for $\Lambda_{UV}^2 = |eH|$ (61) is canonical [23].

The result (61) is readily understood from the fermion loop diagram of Fig. 2 with the fermionic lines corresponding to a constitutive fermion moving in the external magnetic field. The free loop with 2 H-insertions is of the form of H^2/p^4 with p a typical loop momentum. Clearly, the integral diverges both in the ultraviolet and infrared. The cutoff in the ultraviolet is Λ_{UV}, while in the infrared, it is $\sigma + m$ for free constitutive fermions and

$$(\sigma + m)^2 \to |eH| + (\sigma + m)^2 \tag{62}$$

for constitutive fermions in a magnetic field. For $\Lambda_{UV} > \sqrt{|eH|} > (\sigma + m)$ (61) follows, while for $\Lambda_{UV} > (\sigma + m) > \sqrt{|eH|}$, we have

$$\Omega_H(0,0) \approx \frac{H^2}{2}\left(1 + \chi e^2 \ln\left(\frac{\Lambda_{UV}^2}{(\sigma + m)^2}\right)\right). \tag{63}$$

For $\sqrt{|eH|} > (\sigma + m)$, we note that the higher H-insertions in Fig. 2 are increasingly infrared-sensitive making them all of the order of $|eH|^2$. They

renormalize the classical field contribution [23]. In dense matter near the critical points, the UV cutoff in (63) is traded through

$$\Lambda_{\mathrm{UV}}^2 \rightarrow |\omega_0 + i\mu|^2 \tag{64}$$

with $\omega_0 = \pi T$, leading to

$$\Omega_H(T, \mu) \approx \frac{H^2}{2}\left(1 + \chi e^2 \ln\left(\frac{|\omega_0 + i\mu|^2}{|eH| + (\sigma + m)^2}\right)\right) \tag{65}$$

in agreement with detailed limits derived in [23]. (65) permeates all constitutive quark calculations in the context of the magnetic catalysis of chiral symmetry breaking in QCD both in vacuum and matter [9] (and references therein).
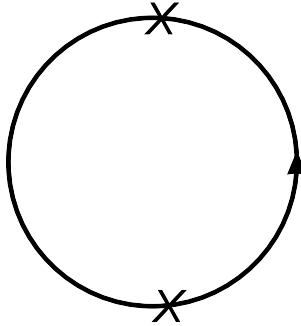

Fig. 2. Magnetic contributions to the constitutive quark loop. See the text.

Our starting point for an RMM analysis of the phase diagram at finite H in matter with twisted boundary conditions is $\Omega = \Omega_M + \Omega_H$. With only H present, the minimum $\partial\Omega/\partial\sigma_* = 0$ using (55) and (65) yields

$$\sigma_* = \Sigma\sqrt{2\boldsymbol{n}_4 + \chi H^2} \tag{66}$$

which is to be compared with (59). This yields a change in the chiral condensate

$$\Delta\Sigma = \frac{\left\langle \Psi_4^\dagger \Psi_4 \right\rangle}{\left\langle \Psi_4^\dagger \Psi_4 \right\rangle_0} = \sqrt{1 + \frac{\chi |eH|^2}{2\boldsymbol{n}_4}} - 1 \tag{67}$$

which is quadratic for low $|eH|$ and linear for intermediately large $|eH|$. We recall that for ultra-strong magnetism at zero temperature, the ratio asymptotes $|eH|^{3/2}$ as both suggested by RMM and perturbative QCD.

The asymptotic of (67)

$$\Delta\Sigma \approx \sqrt{\frac{(\chi/2)}{\boldsymbol{n}_4}}\,|eH| \tag{68}$$

is smaller than (38) by the factor of

$$\sqrt{\chi/2} \approx \sqrt{N_C/24}/\pi \approx 1/10\,. \tag{69}$$

The random matrix model is not restricted by the 1-loop result as it involves the delocalization of the dimensionally reduced chiral quarks through quasi-2-dimensional zero modes and is more in line with the currently reported lattice results. The results of the random matrix analysis are reproduced by setting $\chi \to 2$ in Ω_H. This effective action analysis without boundary twists whether temporal (Polyakov) or spatial (BA), emphasizes the underlying diamagnetic character of the random matrix analysis above when restricted to the LLL.

7. Conclusions and prospects

We have presented a chiral RMM for the analysis of the recent lattice QCD simulations in the presence of a strong QED magnetic field. The results for intermediate values of $|eH| > 1/\rho^2 \approx 0.3\,\mathrm{GeV}^2$ are readily understood through the infrared branch of the LLL which causes the quarks to dimensionally reduce from 4 to 2 dimensions. Quarks trapped in 4-dimensional LLL are more prone to break spontaneously chiral symmetry through random disorder by gluonic configurations whether perturbative or non-perturbative. This is the essence of the magnetic catalysis discussed in [9] (and references therein). Note that our reduction of the spectrum is in quark virtualities not quark energies and, therefore, from $4+1$ to $2+1$ rather than $3+1$ to $1+1$.

In 2 dimensions, the interactions due to the semiclassical vacuum configurations, *i.e.* instantons or calorons cause them to accumulate at zero virtuality. The accumulation is characterized by a level spacing of the order of $1/\sqrt{V_4}$ which is intermediate between $1/V_4$ in the vacuum and $1/^4\sqrt{V_4}$ in a free box. The change in the chiral condensate is shown to increase linearly with $|eH|$ (catalysis) with a slope $1/\sqrt{\boldsymbol{n}_4} \approx 1\,\mathrm{fm}^2$ with $\boldsymbol{n}_4$ the instanton vacuum density. These results are consistent with the current lattice data at zero temperature. For very weak $|eH|$, the gapped charged pions dominate the contribution in the diffusive regime in line with the leading result from chiral perturbation theory. At ultra-strong magnetic fields $|eH| \geq 10/\rho^2 \approx 3\,\mathrm{GeV}^2$, the RMM suggests an increase in the chiral condensate as $|eH|^{3/2}$ in agreement with perturbative QCD estimates for

ultra-strong fields using a Bethe–Salpeter analysis [14]. We note that our estimation of the divide between the strong and ultra-strong regime is only qualitative — we have assumed that about 10 Landau levels fit within the instanton transverse size (see above), which provides only an order of magnitude estimate. If we were to assume that about 20 Landau levels fit the instanton transverse size, the ultrastrong regime will correspond to the value of $6\,\mathrm{GeV}^2$. The largest magnetic fields probed in the lattice simulation corresponds to $3\,\mathrm{GeV}^2$ [12]. At this value, the critical temperature is only weakly dependent on the magnetic field, in agreement with our prediction for (36). This fact may suggest that the ultra-strong regime is not yet accessible by current lattice simulations.

At finite but high temperature, the emergence of a Polyakov holonomy does not affect the decoupling of the LLL. We have shown that a small shift in the trivial part of this holonomy allows for a rapid decrease (anti-catalysis) of the chiral condensate near the critical temperature as suggested recently by lattice simulations [13]. This small change in the Polyakov holonomy is quadratic in the magnetic field. It reflects on the back-reaction of the quarks on the effective potential of the temporal holonomies near the trivial solution.

We have explicitly shown how the random matrix effective action emerges from our analysis in the dimensionally reduced limit. Also, we have provided a specific construction of a number of random matrix inspired models to allow for a simple comparison with current constituent quark models with magnetism such as the NJL models. A more detailed analysis of the phase diagrams emerging from these effective actions will be detailed elsewhere.

In random matrix theory, the spectral distributions in the microscopic limit capture more information on the subtleties of chiral symmetry breaking such as the role of quark representations, quark masses and magnetism and twists.

Of particular interest is $N_C = 2$ with an external magnetic field which upsets time-reversal symmetry, a big deal for this representation. Indeed, for $N_C = 2$ the chiral disorder involves not only the pions (diffusons) but also the baryons (cooperons) both of which are degenerate following the extra Pauli–Gursey symmetry. The cooperon is sensitive to the breaking of time-reversal symmetry because of its charge [21].

Finally, it would be interesting to revisit the role of the number of flavors, quark masses and the spatial and temporal twists on the results we have derived for a more critical comparison with current lattice data. The effect of the chemical potential on the LLL analysis should also shed more light on the role of magnetism on the QCD phase diagram. Some of these issues will be addressed next.

REFERENCES

[1] D. Diakonov, *Prog. Part. Nucl. Phys.* **51**, 173 (2003).

[2] T. Schaefer, E.V. Shuryak, *Rev. Mod. Phys.* **70**, 323 (1998) [arXiv:hep-ph/9610451].

[3] M.A. Nowak, M. Rho, I. Zahed, *Chiral Nuclear Dynamics*, World Scientific, Singapore 1995.

[4] T. Banks, A. Casher, *Nucl. Phys. B* **169**, 103 (1980).

[5] R.A. Janik, M.A. Nowak, G. Papp, I. Zahed, *Phys. Rev. Lett.* **81**, 264 (1998) [arXiv:hep-ph/9803289].

[6] J.C. Osborn, J.J.M. Verbaarschot, *Phys. Rev. Lett.* **81**, 268 (1998).

[7] K. Takahashi, I. Iida, *Nucl. Phys. B* **573**, 685 (2000).

[8] M.E. Berbenni *et al.*, *Nucl. Phys. Proc. Suppl.* **83**, 914 (2000).

[9] I.A. Shovkovy, *Lect. Notes Phys.* **871**, 13 (2013) [arXiv:1207.5081 [hep-ph]].

[10] L. McLerran, arXiv:hep-ph/0311028.

[11] G.S. Bali *et al.*, *J. High Energy Phys.* **1202**, 044 (2012) [arXiv:1111.4956 [hep-lat]]; *Phys. Rev. D* **86**, 071502 (2012) [arXiv:1206.4205 [hep-lat]]; **86**, 094512 (2012) [arXiv:1209.6015 [hep-lat]]; *PoS* **ConfinementX**, 197 (2012) [arXiv:1301.5826 [hep-lat]].

[12] G. Endrodi, *J. High Energy Phys.* **1507**, 173 (2015).

[13] F. Bruckmann, G. Endrődi, T.G. Kovács, *J. High Energy Phys.* **1304**, 112 (2013) [arXiv:1303.3972 [hep-lat]].

[14] I.A. Shushpanov, A.V. Smilga, *Phys. Lett. B* **402**, 351 (1997) [arXiv:hep-ph/9703201].

[15] R.A. Janik, M.A. Nowak, G. Papp, I. Zahed, *Acta Phys. Pol. B* **29**, 3215 (1998) [arXiv:hep-ph/9807467].

[16] J. Gasser, H. Leutwyler, *Phys. Lett. B* **188**, 477 (1987); **184**, 83 (1987).

[17] A.D. Jackson, J.J.M. Verbaarschot, *Phys. Rev. D* **53**, 7223 (1996) [arXiv:hep-ph/9509324].

[18] G. Basar, G.V. Dunne, D.E. Kharzeev, *Phys. Rev. D* **85**, 045026 (2012) [arXiv:1112.0532 [hep-th]].

[19] M. D'Elia, S. Mukherjee, F. Sanfilippo, *Phys. Rev. D* **82**, 051501 (2010); M. D'Elia, F. Negro, *Phys. Rev. D* **83**, 114028 (2011).

[20] J. Jurkiewicz, M.A. Nowak, I. Zahed, *Nucl. Phys. B* **478**, 605 (1996) [*Erratum ibid.* **513**, 759 (1998)] [arXiv:hep-ph/9603308].

[21] R.A. Janik, M.A. Nowak, G. Papp, I. Zahed, *Phys. Lett. B* **440**, 123 (1998); arXiv:hep-ph/9807499; *Nucl. Phys. Proc. Suppl.* **83**, 977 (2000).

[22] S.M. Nishigaki, *Phys. Rev. D* **86**, 114505 (2012) [arXiv:1208.3452 [hep-lat]].

[23] P. Elmfors, P. Liljenberg, D. Persson, B.-S. Skagerstam, *Phys. Rev. D* **51**, 5885 (1995); D. Persson, *Ann. Phys.* **252**, 33 (1996) [arXiv:hep-ph/9601259].

[24] P.N. Meisinger, M.C. Ogilvie, *Phys. Lett. B* **407**, 297 (1997) [arXiv:hep-lat/9703009].

[25] M.A. Stephanov, *Phys. Lett. B* **375**, 249 (1996) [arXiv:hep-lat/9601001].